Validation and test of a novel multi-input converter in extreme conditions using PSOPIC in hybrid power generation environment

Supriya Jayaprakash[1], Rajashekar Jangam Siddamallaiah[2]
[1]Department of Electrical and Electronics Engineering, Dayananda Sagar College of Engineering, Bangalore, India
[2]Department of Electronics and Instrumentation Engineering, Dayananda Sagar College of Engineering, Bangalore, India

Article Info

Article history:

Received Aug 13, 2023
Revised Nov 25, 2023
Accepted Dec 7, 2023

Keywords:

Fuel cell power generation
Multi-port-SEPIC converter
PSO-PI control
Photovoltaic power generation
Wind power generation

ABSTRACT

The need for renewable energy resources increases due to the day-by-day increase in load demand. Still, there is a need for new technology to operate the existing power system optimally. Distributed generation (DGENs) are helpful in meeting the demand of power due to its lower cost compared to the construction of the complete power system. But this DGEN is constructed using renewable resources, which are intermittent in nature. So, hybrid power generation, which uses multiple sources, is used to satisfy the power need. In this paper, validation, and test of a new multi-input single ended primary inductor converter (MI-SEPIC) is proposed. The performance of the MI-SEPIC converter is tested by connecting photovoltaic (PV), wind, and fuel cells. The proposed system is connected to the grid, and the power transients are analyzed. The direct quadrature (DQ) control of grid synchronization is discussed in this paper. The conventional PI controller is replaced with a hybrid particle swarm optimization tuned proportional integral control (PSOPIC), and the results are compared. Verification is done using MATLAB software. Validation and test with different test cases to prove the sturdiness of the complete system is explained.

This is an open access article under the CC BY-SA license.

Corresponding Author:

Supriya Jayaprakash
Department of Electrical and Electronics Engineering, Dayananda Sagar College of Engineering
Bangalore, Karnataka, India
Email: supriya-eee@dayanandasagar.edu

1. INTRODUCTION

The important role is to adjust for power usage to maintain voltage control. The photovoltaic (PV) power control with grid are mostly discussed in [1]–[5]. The grid's dynamic voltage stability with PV is described in [6]. Performance comparison of maximum power point tracking (MPPT) algorithms [7]. The Z-source inverter's PV-based grid connection control uses fuzzy logic [8]. Doing so should boost voltage. Fuzzy logic proportional integral controller (PIC) adjustments are shown in [9]–[11], while [12] analyses confusing implementation literature. This study examines grid-coupled PV system in reduction of power disturbance, improvement of stability and reduction of total harmonic distortion. It also investigates ways to improve the PIC, which is being replaced by fuzzy-PIC [13] and the next ANFIS-PIC. The next paragraphs suggest multi-input converters (MICs).

A full MIC construction plan is in [14]. A converter topology-based MIC synthesis approach was devised. Connecting an appropriate pulse current or voltage source to a converter improves device performance. A new multi-port converter is proposed in [15]. This can work as both boost and buck operation. Both positive input and electricity pass through this bidirectional converter. A hybrid PV-battery-fuel cell power system using a multi-port converter is detailed in [16]. A MIC bidirectional with a good step-up ratio and efficiency is suggested by [17]. The converter can operate in standalone, united power supply and discharge/charge modes.

Preview study [18] offers a 3-port converter with optimized converter architecture for solar power systems which is standalone. This concept seeks to boost system efficiency and cost saving. A unique MIC buck and boost converter for street lights is described in [19]. A unitary converter with multi-input with unidirectional power ports and a storage element port describes in [20]. The proposed system has four power switches with four duty cycles each. Non-inverting boost converter [21] is made without isolation and multi-input with multi-output. In this converter, the user can divide load power across input sources as desired. A converter with z-source with MIC characteristics with the same amount of capacitors and inductors proposed in [22]. MICs are used in another hybrid energy conversion approach [23]. Modifying current issues presents several new topologies [24], [25].

Multi-input single ended primary inductor converter (MI-SEPIC) is proposed in the work [26]. Connecting PV, wind, and fuel cells tests MI-SEPIC converter performance. Power oscillations are evaluated when the system proposed is grid-connected. This study examines direct quadrature (DQ) grid synchronization control. A normal PIC is replaced with a PSO-tuned one to compare results.

2. METHOD

Here proposed the new MI-SEPIC converter. The proportional integral controller (PIC) is replaced with particle swarm optimization tuned proportional integral control (PSOPIC) to improve the power oscillation in direct quadrature (DQ) control. The Figure 1 shows the proposed technique, where Figure 2 shows the block diagram of the proposed MI-SEPIC. The controller connections also given clearly. The grid side converter is the three-phase converter with six switches.

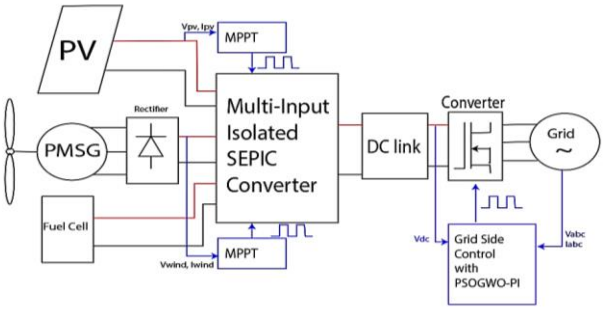

Figure 1. Proposed power generation model

2.1. DQ controlled grid tie controller

The grid side controller is made with DQ control. DQ control is a tranformation which uses the formula for converting the ABC to DQ and viceversa. The park's transformation shows in (1). The inverse park transformation shows in (2). Here, 'u' can be voltage 'V' or current 'I'. Based on (1) and (2) are common for V & I.

$$\begin{pmatrix} u_d \\ u_q \\ u_0 \end{pmatrix} = \begin{pmatrix} \cos(\omega t) & \cos\left(\omega t - \frac{2\pi}{3}\right) & \cos\left(\omega t + \frac{2\pi}{3}\right) \\ -\sin(\omega t) & -\sin\left(\omega t - \frac{2\pi}{3}\right) & \sin\left(\omega t + \frac{2\pi}{3}\right) \\ \frac{1}{2} & \frac{1}{2} & \frac{1}{2} \end{pmatrix} \begin{pmatrix} u_a \\ u_b \\ u_c \end{pmatrix} \tag{1}$$

$$\begin{pmatrix} u_d \\ u_q \\ u_0 \end{pmatrix} = \begin{pmatrix} \cos(\omega t) & -\sin(\omega t) & 1 \\ -\sin(\omega t) & -\sin\left(\omega t - \frac{2\pi}{3}\right) & 1 \\ \cos\left(\omega + \frac{2\pi}{3}\right) & -\sin\left(\omega t + \frac{2\pi}{3}\right) & 1 \end{pmatrix} \begin{pmatrix} u_a \\ u_b \\ u_c \end{pmatrix} \tag{2}$$

Figure 3 shows the DC voltage regulation which generated the current reference shown in Figure 4 and controlled with PSOPIC.From the voltage reference and measured values given to the PI controller as error. This error is converted as diret current. And the current measurements are converted to direct and quadratic voltages using PSOPIC controller.

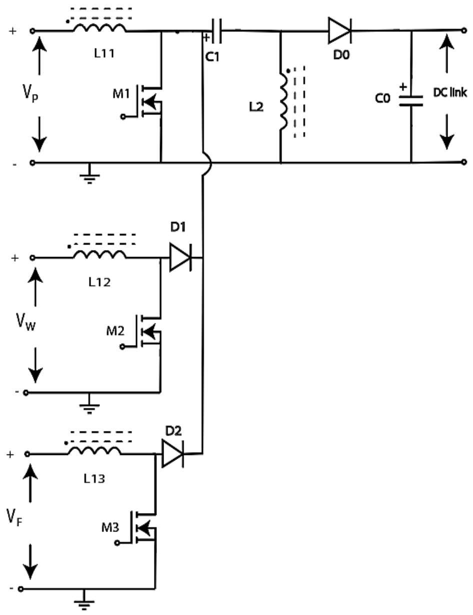

Figure 2. New MI-SEPIC circuit [26]

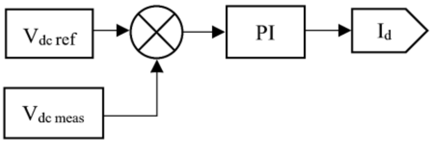

Figure 3. DC voltage regulation using PIC

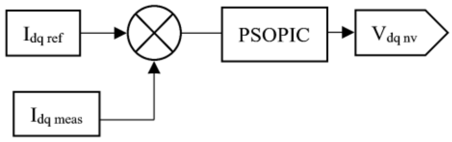

Figure 4. PSOPIC based current regulation

2.2. Current regulator designed with PI and PSO-PI

In general, PIC are used in current regulation of electrical sytems. The output of the conventional current regulator is expressed in (3).

$$Out(t) = K_p\left(I_{dq}{}^{*} - I_{dq}\right) + K_i \int (I_{dq}{}^{*} - I_{dq})dt \quad (3)$$

Where $I_{dq}*$ reference current I_{dq} - the measured current. It is the responsibility of the PIC to make an effort to reduce the inaccuracy that is caused by the disparity between them. The output is the signal that is advised to be used since it has the fewest number of mistakes (out(t)). While the integral constant is denoted by the letter Ki, the proportional constant refers to Kp. In order to make adjustments to the parameters Kp and Ki, manual tuning processes are utilised. Block schematic of PSOPIC-based current regulation is depicted in Figure 5, which may be found here. Each of the outputs is added together and then presented as output.

2.3. Problem formulation

The objective function used here is settling time minimization. The settling time value from the Simulink diagram is measured using the MATLAB command. The settling time values stored in the workspace. The final value of the settling time is taken here as the objective function. It can be represented as (4).

$$f\left(k_p, k_i\right) = \text{minimize } (settling\ time\ (s)) \quad (4)$$

The inequality constraints are given as (5) and (6).

$$0 < k_p < 1200 \quad (5)$$

$$0 < ki < 1200 \quad (6)$$

The values of the final results from the simulation was not much when kp and ki varied more than 1200. So the maximum value is selected here as 1200. The Figure 6 shows the flowchart of the PSOPIC. The initialization has the KP, KI, C1, and C2 are shown and then the evaluation of the fitness function is done. The KP and KI values are populated in random manner, (5) and (6) are responsible for it. Then the random values one by one placed in the simulation and the settling time is calculated. The settling time for each KP and KI are listed and minimum is taken. This one is taken as best values and then the PSO algorithm repopulates the values and then evaluates the fitness for the next iteration. Till the final iteration the optimal values are found.

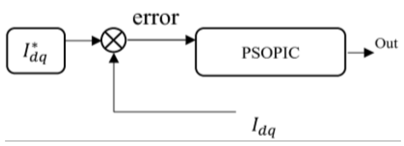

Figure 5. PSOPIC control of current regulation

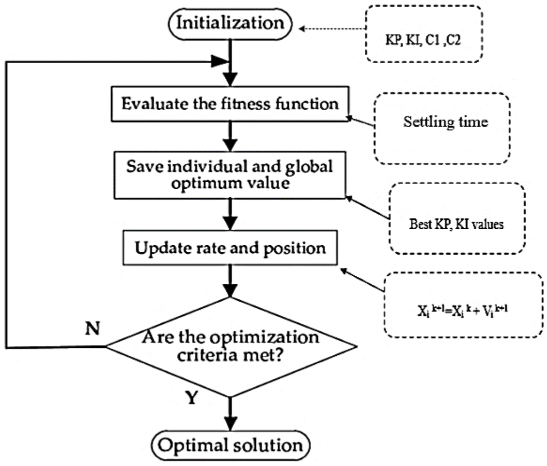

Figure 6. PSOPIC flow chart

3. RESULTS AND DISCUSSION

As sources of power wind power generation, PV power and fuel cell power generation are each utilized. DC power is generated by photovoltaic cells and fuel cells in this context. The generation of wind power is accomplished by the use of permanent-magnet synchronous motor (PMSM) generators, which generate high frequency AC power. By utilizing the diode rectifier bridge, this is transformed into direct current. It is the MI-SEPIC converter that receives these specific supplies. During the boosting process, the MPPT algorithm is used to the converter switch. This is exclusively done for wind and photovoltaic energy. The traditional P & O method is considered to be the MPPT methodology that is utilized. Following this, the inverter is connected to the DC link, and the output of the inverter is connected to the electricity grid once it has been connected. Through the use of the DQ approach, the inverter is controlled. In this case, the direct Id and Iq are both under the control of the DQ controller. There is a connection between the electrical grid and a utility load of 1000 kW. Once this need has been met, the grid will then take the electricity that is available in excess of what is required. The simulation's parameters are listed in Table 1, which may be found here. Various tests are taken to prove the proposed concept is stable. The test cases are shown as: i) case 1: sudden load change in the system, ii) case 2: AC side fault, and iii) case 3: DC side fault.

Figure 7 shows the DC link voltage in V. It shows the settling is faster in PSOPIC compared with PI. Figure 8 shows the load change in the system. The load change has oscillation in the beginning of the waveform. Figure 9 shows the measured solar power. Here also the PSOPIC is faster and Figure 9 shows that the oscillations in the power also reduced. Figure 10 shows the zoomed Figure 9. Figure 11 shows the fuel cell measured power. It shows the PSOPIC is faster in settled and stability is good compared to PI. Figure 12 shows the wind power measured power. It shows the oscillations are less in PSOPIC. Figure 13 zoomed view of Figure 12. Table 2 shows the response time comparison. Table 3 shows the settling time comparison. Figure 12 shows the response time comparison.

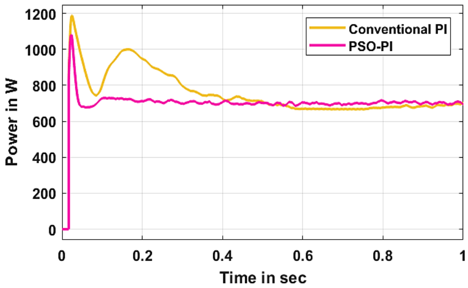

Figure 7. DC link voltage in V

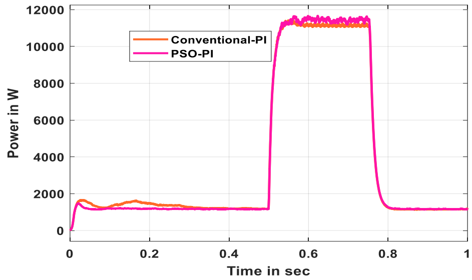

Figure 8. Load change in the system

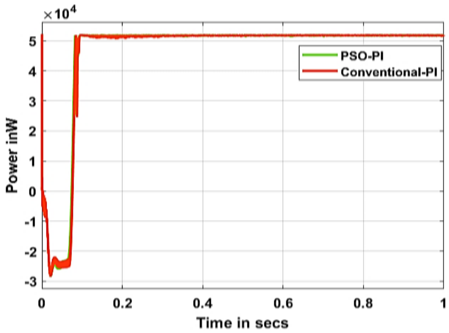

Figure 9. Measured solar power

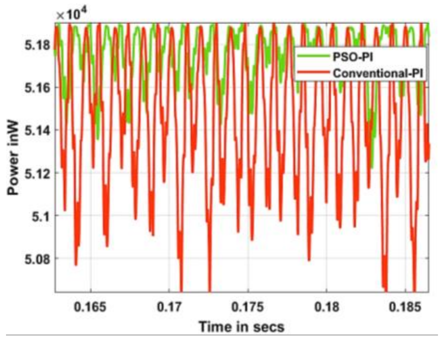

Figure 10. Zoomed of figure 9

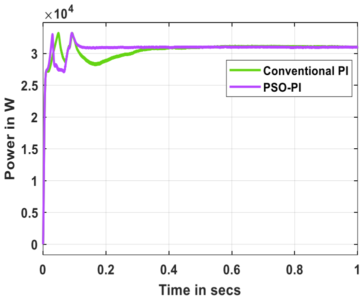

Figure 11. Fuel cell measured power

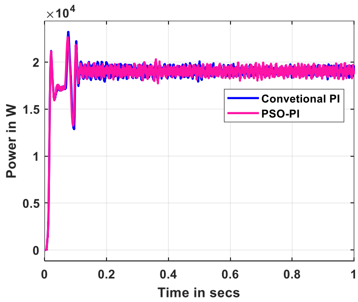

Figure 12. Wind power measured power

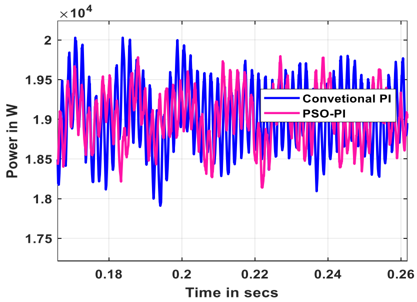

Figure 13. Zoomed view of Figure 12

Table 1. Parameters used for simulation

Parameters	Module type	SunPower SPR-305-WHT	Parameters	Type	PEMFC
PV power plant	Number of series connected modules per string	5	Fuel Cell	Power (W)	6
	Number of parallel connected modules per string	34		Voltage (V)	45
	Open circuit voltage (V)	64.2		Series connected fuel cells	4
	Short circuit current (A)	5.96		Nominal power in W	24 kW
	Maximum power point voltage (V)	54.7	Grid	Voltage (V)	0.4 kV
	Maximum power point current (A)	5.58		Frequency (Hz)	50 Hz
	Nominal power in W	51.8 kW	Transformer	Nominal power in W	100 kW
Wind power plant	Nominal mechanical power (W)	20 kW		Primary voltage	0.4 kV
	Base wind speed (m/s)	12		Secondary voltage	11 kV
	Maximum power at base wind speed	0.73	Filter	R	2 mohm
	Number of turbines	3		L	1.5 mH
	Torque in Nm	6	MI-SEPIC	L11, L12, L13	5 mH
	DC voltage rating (V)	600		C1	12 uF
	Speed in RPM	4500		L2	5 mH
				Co	12000 uF

Table 2. Response time comparison

Test cases	Conventional PI in secs	PSOPIC in secs
Case 1	0.1	0.06
Case 2	0.1	0.07
Case 3	0.1	0.06

Table 3. Settling time comparison in secs

Test cases	Conventional PI in secs	PSOPIC in secs
Case 1	0.5	0.11
Case 2	0.5	0.12
Case 3	0.5	0.12

4. CONCLUSION

In the course of this research, the testing and validation of MI-SEPIC is suggested. In order to analyses the performance of the MI-SEPIC converter, photovoltaic, wind, and fuel cell connections are necessary. The power oscillations are analyzed as it is connected to the grid. In this study, grid synchronization control in DQ mode is the subject of discussion. The PSOPIC standard is used as a point of comparison with the traditional PIC. A comparison is made between the outcomes when a PSOPIC is used in place of a normal PI. At this point, a MATLAB simulation is being executed with the intention of validating the proposed system. The results demonstrate that the method that was proposed is superior to the method that was traditionally used.

REFERENCES

[1] R. Guerrero-Lemus, D. Cañadillas-Ramallo, T. Reindl, and J. M. Valle-Feijóo, "A simple big data methodology and analysis of the specific yield of all PV power plants in a power system over a long time period," *Renewable and Sustainable Energy Reviews*, vol. 107, pp. 123–132, Jun. 2019, doi: 10.1016/j.rser.2019.02.033.

[2] P. Han, Z. Lin, L. Wang, G. Fan, and X. Zhang, "A survey on equivalence modeling for large-scale photovoltaic power plants," *Energies*, vol. 11, no. 6, p. 1463, Jun. 2018, doi: 10.3390/en11061463.

[3] I. de la Parra, M. Muñoz, E. Lorenzo, M. García, J. Marcos, and F. Martínez-Moreno, "PV performance modelling: A review in the light of quality assurance for large PV plants," *Renewable and Sustainable Energy Reviews*, vol. 78, pp. 780–797, Oct. 2017, doi: 10.1016/j.rser.2017.04.080.

[4] M. Mehrasa, E. Pouresmaeil, A. Sepehr, B. Pournazarian, M. Marzband, and J. P. S. Catalão, "Control technique for the operation of grid-tied converters with high penetration of renewable energy resources," *Electric Power Systems Research*, vol. 166, pp. 18–28, Jan. 2019, doi: 10.1016/j.epsr.2018.09.015.

[5] M. Mehrasa, E. Pouresmaeil, H. Soltani, F. Blaabjerg, M. Calado, and J. Catalão, "Virtual inertia and mechanical power-based control strategy to provide stable grid operation under high renewables penetration," *Applied Sciences*, vol. 9, no. 6, p. 1043, Mar. 2019, doi: 10.3390/app9061043.

[6] D. Wang, K. Meng, X. Gao, J. Qiu, L. L. Lai, and Z. Y. Dong, "Coordinated dispatch of virtual energy storage systems in LV grids for voltage regulation," *IEEE Transactions on Industrial Informatics*, vol. 14, no. 6, pp. 2452–2462, Jun. 2018, doi: 10.1109/TII.2017.2769452.

[7] S. S. Refaat, H. Abu-Rub, A. P. Sanfilippo, and A. Mohamed, "Impact of grid-tied large-scale photovoltaic system on dynamic voltage stability of electric power grids," *IET Renewable Power Generation*, vol. 12, no. 2, pp. 157–164, Feb. 2018, doi: 10.1049/iet-rpg.2017.0219.

[8] Y. Chaibi, A. Allouhi, M. Salhi, and A. El-jouni, "Annual performance analysis of different maximum power point tracking techniques used in photovoltaic systems," *Protection and Control of Modern Power Systems*, vol. 4, no. 1, p. 15, Dec. 2019, doi: 10.1186/s41601-019-0129-1.

[9] H. A. Mosalam, R. A. Amer, and G. A. Morsy, "Fuzzy logic control for a grid-connected PV array through Z-source-inverter using maximum constant boost control method," *Ain Shams Engineering Journal*, vol. 9, no. 4, pp. 2931–2941, Dec. 2018, doi: 10.1016/j.asej.2018.10.001.

[10] H. Anantwar, D. B. R. Lakshmikantha, and S. Sundar, "Fuzzy self tuning PI controller based inverter control for voltage regulation in off-grid hybrid power system," *Energy Procedia*, vol. 117, pp. 409–416, Jun. 2017, doi: 10.1016/j.egypro.2017.05.160.

[11] H. W. D. Hettiarachchi, K. T. M. U. Hemapala, and A. G. B. P. Jayasekara, "Review of applications of fuzzy logic in multi-agent-based control system of AC-DC hybrid microgrid," *IEEE Access*, vol. 7, pp. 1284–1299, 2019, doi: 10.1109/ACCESS.2018.2884503.

[12] Q. Zhu, X. Zhong, and B. Xu, "Design of Fuzzy-PI compound control system for three-cylinder hydraulic parallel robot," in *2007 International Conference on Mechatronics and Automation*, Aug. 2007, pp. 989–993. doi: 10.1109/ICMA.2007.4303682.

[13] B. G. Sujatha and A. G. S., "Grid synchronisation of photovoltaic distributed generation using hybrid FUZZY-PI controller," *International Journal of Innovative Technology and Exploring Engineering*, vol. 9, no. 1, pp. 5385–5390, Nov. 2019, doi: 10.35940/ijitee.A4740.119119.

[14] Y.-C. Liu and Y.-M. Chen, "A systematic approach to synthesizing multi-input DC–DC converters," *IEEE Transactions on Power Electronics*, vol. 24, no. 1, pp. 116–127, Jan. 2009, doi: 10.1109/TPEL.2008.2009170.

[15] A. Khaligh, J. Cao, and Y.-J. Lee, "A multiple-input DC–DC converter topology," *IEEE Transactions on Power Electronics*, vol. 24, no. 3, pp. 862–868, Mar. 2009, doi: 10.1109/TPEL.2008.2009308.

[16] S. H. Hosseini, S. Danyali, F. Nejabatkhah, and S. A. K. Mozafari Niapoor, "Multi-input DC boost converter for grid connected hybrid PV/FC/Battery power system," in *2010 IEEE Electrical Power & Energy Conference*, Aug. 2010, pp. 1–6. doi: 10.1109/EPEC.2010.5697177.

[17] R.-J. Wai, C.-Y. Lin, and Y.-R. Chang, "High step-up bidirectional isolated converter with two input power sources," *IEEE Transactions on Industrial Electronics*, vol. 56, no. 7, pp. 2629–2643, Jul. 2009, doi: 10.1109/TIE.2009.2018427.

[18] Y. Hu, W. Xiao, W. Cao, B. Ji, and D. J. Morrow, "Three-port DC–DC converter for stand-alone photovoltaic systems," *IEEE Transactions on Power Electronics*, vol. 30, no. 6, pp. 3068–3076, Jun. 2015, doi: 10.1109/TPEL.2014.2331343.

[19] S. H. Hosseini, S. K. Haghighian, S. Danyali, and H. Aghazadeh, "Multi-input dc boost converter supplied by a hybrid PV/Wind turbine power systems for street lighting application connected to the grid," in *2012 47th International Universities Power Engineering Conference (UPEC)*, Sep. 2012, pp. 1–6. doi: 10.1109/UPEC.2012.6398632.

[20] F. Nejabatkhah, S. Danyali, S. H. Hosseini, M. Sabahi, and S. M. Niapour, "Modeling and control of a new three-input DC–DC boost converter for hybrid PV/FC/battery power system," *IEEE Transactions on Power Electronics*, vol. 27, no. 5, pp. 2309–2324, May 2012, doi: 10.1109/TPEL.2011.2172465.
[21] A. Nahavandi, M. T. Hagh, M. B. B. Sharifian, and S. Danyali, "A nonisolated multiinput multioutput DC–DC boost converter for electric vehicle applications," *IEEE Transactions on Power Electronics*, vol. 30, no. 4, pp. 1818–1835, Apr. 2015, doi: 10.1109/TPEL.2014.2325830.
[22] S. M. Dehghan, M. Mohamadian, A. Yazdian, and F. Ashrafzadeh, "A dual-input–dual-output Z-source inverter," *IEEE Transactions on Power Electronics*, vol. 25, no. 2, pp. 360–368, Feb. 2010, doi: 10.1109/TPEL.2009.2028345.
[23] A. Khaligh, "A multiple-input dc-dc positive buck-boost converter topology," in *2008 Twenty-Third Annual IEEE Applied Power Electronics Conference and Exposition*, Feb. 2008, pp. 1522–1526. doi: 10.1109/APEC.2008.4522926.
[24] S. Padmakala, S. Gomathi, A. Akilandeswari, M. R. F. Banu, S. Padmapriya, and M. Gnanaprakash, "Enhancement of modified multiport boost converter for hybrid system," in *2021 International Conference on Innovative Computing, Intelligent Communication and Smart Electrical Systems (ICSES)*, Sep. 2021, pp. 1–6. doi: 10.1109/ICSES52305.2021.9633853.
[25] P. L. Santosh Kumar Reddy and Y. P. Obulesu, "Design and development of a new transformerless multi-port DC–DC boost converter," *Journal of Electrical Engineering & Technology*, vol. 18, no. 2, pp. 1013–1028, Mar. 2023, doi: 10.1007/s42835-022-01145-9.
[26] S. Jayaprakash and R. J. Siddamallaiah, "A novel multi-port SEPIC converter with grid-tie system for hybrid power generation," *International Journal of Power Electronics and Drive Systems (IJPEDS)*, vol. 14, no. 3, pp. 1675–1683, Sep. 2023, doi: 10.11591/ijpeds.v14.i3.pp1675-1683.

BIOGRAPHIES OF AUTHORS

Supriya Jayaprakash currently working as assistant professor in Department of Electrical and Electronics Engineering, Dayananda Sagar College of Engineering, Bangalore. Her area of interest is power electronics, control systems, network analysis, and renewable energy sources. She is pursuing part time Ph.D. in multiport DC-DC converter. She can be contacted at email: supriya-eee@dayanandasagar.edu.

Rajashekar Jangam Siddamallaiah currently working as professor and head of the Department of Electronics and Instrumentation Engineering, Dayananda Sagar College of Engineering, Bangalore. His area of interest is process instrumentation and control. He has many publications in reputed journals. He can be contacted at email: rajashekhar-eie@dayanandasagar.edu.